Biol Cybern (2014) 108:321–336
DOI 10.1007/s00422-014-0600-z

ORIGINAL PAPER

Biological Cybernetics

A parsimonious oscillatory model of handwriting

Gaëtan André · Viviane Kostrubiec · Jean-Christophe Buisson · Jean-Michel Albaret · Pier-Giorgio Zanone

Received: 22 February 2013 / Accepted: 24 March 2014 / Published online: 10 April 2014

Abstract We propose an oscillatory model that is theoretically parsimonious, empirically efficient and biologically plausible. Building on Hollerbach's (Biol Cybern 39:139–156, 1981) model, our Parsimonious Oscillatory Model of Handwriting (POMH) overcomes the latter's main shortcomings by making it possible to extract its parameters from the trace itself and by reinstating symmetry between the x and y coordinates. The benefit is a capacity to autonomously generate a smooth continuous trace that reproduces the dynamics of the handwriting movements through an extremely sparse model, whose efficiency matches that of other, more computationally expensive optimizing methods. Moreover, the model applies to 2D trajectories, irrespective of their shape, size, orientation and length. It is also independent of the end-effectors mobilized and of the writing direction.

Keywords Graphonomics · Coordination dynamics · Oscillations · Motor pattern · Handwriting

1 Introduction

Handwriting can be regarded as the ultimate motor skill. Through one of the longest learning processes known to humans, it achieves the exquisite and sophisticated coordination of a great number of components, not only from the hand and the forearm, the endeffectors for the trace, but also from the entire body, determining a whole posture which has noticeable effects on the written production (Blöte et al. 1987; Sassoon 1993). As such, handwriting provides scientists with a unique experimental window into motor expertise and its acquisition.

A survey of the literature yields numerous models that capture several features of trajectory formation, hence the handwriting movements. They can roughly be classified into two categories: discrete and continuous models. Discrete models apply some optimization algorithms over a segment of the trace defined as a stroke according to more or less arbitrary criteria (Edelman and Flash 1987; Bullock et al. 1993; Teulings 1996; Plamondon and Djioua 2006). A stroke represents a basic movement unit, of varying length and shape, executed by the motor system in a feedforward control mode. Teulings (1996) captured the notion of movement unit with the term 'ballistic stroke.' The process of handwriting itself may be then viewed as the concatenation of strokes in space and time. This piecemeal process involves a graphic motor buffer where the corresponding motor patterns or engrams (e.g., Viviani and Terzuolo 1982) extracted from a memory store are eventually translated into appropriate neural commands to the muscles (Ellis 1982; Patterson and Wing 1989).

The incertitude about the definition of what a stroke is hampers discrete models of handwriting. The first issue pertains to the size of a stroke. Depending on the task and the writer's skill, it may be a small fragment of trajectory, a letter, a grapheme or even a word (Wing 1978; Teulings et al. 1986; Kandel and Spinelli 2010). The second issue pertains to the concatenation process between successive strokes. At times, the units tend to smudge into each other, a phenomenon called coarticulation; at other times, they appear to be connected by an additional segment of trajectory (Meulen-

G. André · J.-C. Buisson (✉)
UPS, CNRS, IRIT UMR 5505, University of Toulouse, Toulouse, France
e-mail: buisson@enseeiht.fr

G. André
e-mail: gaetan.andre@irit.fr

V. Kostrubiec · J.-M. Albaret · P.-G. Zanone
UPS, PRISSMH EA 4561, University of Toulouse, Toulouse, France
e-mail: pier-giorgio.zanone@univ-tlse3.fr

broek and Galen 1989). Such variability in size, shape and timing undermines a robust determination of the nature, features and properties of a stroke, lessening by the same token its plausibility.

Continuous models on the contrary posit that the trace is the outcome of a nonstop generative process, usually oscillatory, which is modulated parametrically every now and then in a mode that mixes feedback and feedforward control (e.g., Stark 1968). The mixed process merges feedforward mechanisms of generation with feedback mechanisms of updating, so that the desired trajectory be obtained. In a seminal paper, Hollerbach (1981) made a first account of continuous trajectory formation in handwriting as a combination of the motion of two linear oscillators, deemed to capture the motion of wrist and fingers. The model basically assumed that each antagonist muscle pair about the joints behaves as a harmonically moving mass-spring system. Handwriting is thus generated through the combined action of the pair of oscillators set in an orthogonal fashion, generating oscillation in the horizontal and vertical directions. The addition of a translational motion from left to right at a constant speed, typical of most western scripts, separates the strokes/letters spatially. However, crude and incomplete the model may be, it still provides a very sparse mechanism for trace generation: A large number of different graphic shapes can be obtained by intermittently updating a limited set of parameters, namely the amplitude, the frequency and the phase of each oscillator.

Strangely enough, this proposal has not been followed by much theoretical work (except for Singer and Tishby 1994, who made but a cursory reference thereto). More recently, a series of empirical work tested an extension of the oscillatory model proposing that handwriting emerges from the nonlinear coupling between the orthogonal oscillators (Athènes et al. 2004). Due to this nonlinearity, several stable modes of synchronization between the oscillators were expected to arise, according to the principles of dynamic pattern theory (Kelso 1984, 1995; Schöner and Kelso 1988). In a task demanding participants to draw several ellipses of various eccentricities, Athènes and colleagues showed that a straight line and an ellipse with an intermediate eccentricity were produced with high accuracy and velocity, independent of their orientation. They concluded that such preferences resulted from the stability of some synchronization modes between the oscillators arising from their mutual coupling. This view afforded specific predictions about the degradation of handwriting in deleterious situations (Sallagoïty et al. 2004).

Building on the above theoretical and empirical work, the present article offers a model for 2D trajectory formation in humans, probably a valid blueprint of any graphic skills, including handwriting. In the following, we shall introduce a Parsimonious Oscillatory Model of Handwriting (POMH), emphasize its computational simplicity, compare its efficiency quantitatively with the existing model of Edelman and Flash (1987) and evaluate its performance on real handwriting of increasing complexity: letters, words, sentences and signatures.

2 An improved oscillatory model of handwriting

2.1 The Hollerbach model

In the Hollerbach (1981) model, handwriting is seen as the result of two superimposed oscillators moving along two distinct directions of the plane: x and y. Although any non-sinusoidal oscillators could work as well, a harmonic function is fairly compatible with the mass-spring dynamics of the endeffectors. The equation of motion for each oscillator is defined as:

$$\dot{x} = a\sin(\omega_x t + \phi_x) + c \tag{1}$$

$$\dot{y} = b\sin(\omega_y t + \phi_y) \tag{2}$$

Where a and b are the horizontal and vertical velocity amplitudes, $\omega_x, \omega_y, \phi_x$ and ϕ_y are, respectively, the frequencies and the phases associated with these oscillators. The parameter c models the constant translation movement to the right when writing. The x axis is thus oriented in this left to right writing direction, whereas the y axis, not necessarily orthogonal to x, can be defined as the slant direction. The model parameters (i.e., a, b, ω_x, ω_y, ϕ_x and ϕ_y) are piecewise constant; they are supposed to be updated only when the vertical velocity is null. Stemming from this formalism, the slant angle β can be expressed as:

$$\tan\beta = \frac{b}{a\cos\phi} \quad \text{where } \phi = \phi_x - \phi_y \tag{3}$$

Another issue pertains to the horizontal velocity value when vertical velocity is null:

$$\Psi = \dot{x}(t_{\dot{y}_0}) = c - a\sin\phi \tag{4}$$

The sign and magnitude of this value indicates the particular shape of the trace at this point. If Ψ is close to zero, then the top corner looks sharp. If it is positive, the top corner becomes rounded. Conversely, a negative value of Ψ results in a full loop. These effects are illustrated in Fig. 1.

Fig. 1 In Hollerbach's model (1981), the shape of the top corners depends on the sign and magnitude of Ψ (see text for further details). **a** $\Psi = 1.2$, **b** $\Psi = -43$, **c** $\Psi = 37$

2.2 Reasons for improving the Hollerbach model

Hollerbach's model calls for improvement because three issues are not addressed.

The main computational drawback of Hollerbach's model lies in the lack of any parameters extraction method from a given handwritten trace. With the assumed asymmetric equations, any such algorithm would involve a nonlinear curve-fitting problem, calling for computationally expensive optimization methods. Our aim is to present here a much more efficient algorithm, stemming from our symmetric choice of the moments when parameters are allowed to change.

Secondly, the c parameter, representing the constant drift of the hand from left to right during writing, is quite ad hoc and unnecessary. Moreover, it imposes the x-axis to be exactly aligned with the writing direction and introduces a dissymmetry between x and y. We will show that it can be simply omitted and that the drift can be accounted for by cumulating phase values between cycles.

Finally, the simultaneous updating of x and y parameters, occurring when the y velocity is null, renders the Hollerbach model similar to a stroke-by-stroke, piecemeal method for trace generation. Even though each stroke is formed via continuous harmonic movements on x and y, it is simply concatenated to the next, which may be very different in shape, leading thereby to undesired angularities at the junction points. We will show below how our improved model overcomes this problem.

2.3 The POMH model

Our model (POMH), compared to Hollerbach's, is simpler because it is symmetric in x and y. The model benefits are as follows: a complete independence from any spatial coordinate system; an analytic solution for extracting parameters from the trace, hence an inexpensive computation; a generation of any 2D trajectory preserving the biological movement dynamics. The POMH model is described in the following paragraphs.

2.3.1 Cinematic equations

We use canonical orthogonal directions of the plan space as axes for the two oscillators. The movements on the x and y axes are defined by:

$$\dot{x} = a_x(t)\sin(\omega_x(t).t + \phi_x(t)) \tag{5}$$
$$\dot{y} = a_y(t)\sin(\omega_y(t).t + \phi_y(t)) \tag{6}$$

where $a_x, \omega_x, \phi_x, a_y, \omega_y, \phi_y$ are constant-by-part functions defined by a parameter series described in 2.3.2.

2.3.2 Parameter series

Let $t_{x,1}, \ldots, t_{x,N_x}$ be the moments of zero velocity on the x-axis, and $t_{y,1}, \ldots, t_{y,N_y}$ the moments of zero velocity on the y-axis. We compute the following elements:

$$\omega_{x,i} = \frac{\pi}{t_{x,i+1} - t_{x,i}} \tag{7}$$
$$\phi_{x,i} = -\frac{\pi t_{x,i}}{t_{x,i+1} - t_{x,i}} \tag{8}$$
$$a_{x,i} = \frac{\pi}{2} mean\,(\dot{x})_{[t_{x,i}, t_{x,i+1}[} \tag{9}$$
$$\omega_{y,i} = \frac{\pi}{t_{y,i+1} - t_{y,i}} \tag{10}$$
$$\phi_{y,i} = -\frac{\pi t_{y,i}}{t_{y,i+1} - t_{y,i}} \tag{11}$$
$$a_{y,i} = \frac{\pi}{2} mean\,(\dot{y})_{[t_{y,i}, t_{y,i+1}[} \tag{12}$$

where *mean* is the mean on the interval $[t_{y,i}, t_{y,i+1}[$.

The functions $a_x, \omega_x, \phi_x, a_y, \omega_y, \phi_y$ are defined by:

$$a_x(t) = a_{x,i} \quad t_{x,i} \le t \le t_{x,i+1} \tag{13}$$
$$\omega_x(t) = \omega_{x,i} \quad t_{x,i} \le t \le t_{x,i+1} \tag{14}$$
$$\phi_x(t) = \phi_{x,i} \quad t_{x,i} \le t \le t_{x,i+1} \tag{15}$$
$$a_y(t) = a_{y,i} \quad t_{y,i} \le t \le t_{y,i+1} \tag{16}$$
$$\omega_y(t) = \omega_{y,i} \quad t_{y,i} \le t \le t_{y,i+1} \tag{17}$$
$$\phi_y(t) = \phi_{y,i} \quad t_{y,i} \le t \le t_{y,i+1} \tag{18}$$

Finally, a trace is completely modeled by the two series:

$$(t_{x,i}, a_{x,i}, \omega_{x,i}, \phi_{x,i}) \quad 1 \le i < N_x \tag{19}$$
$$(t_{y,i}, a_{y,i}, \omega_{y,i}, \phi_{y,i}) \quad 1 \le i < N_y \tag{20}$$

Figure 2 shows the x and y position (middle panels) and velocity (bottom panels) profiles on a sample trace 'umbrella' (upper panel). Circle (resp. square) dot indicate moments when x (resp. y) velocity is null.

2.4 Mathematical justification of computations

2.4.1 Computation of ω and ϕ

Between two successive zeros $t_{x,i}$ and $t_{x,i+1}$ of the velocity on x, the function $\dot{x}$ performs half a period of the sinus function, so:

$$t_{x,i+1} - t_{x,i} = \frac{\pi}{\omega_{x,i}} \text{ and } \omega_{x,i} t_{x,i} + \phi_{x,i} = 0 \tag{21}$$

Similarly on the y-axis:

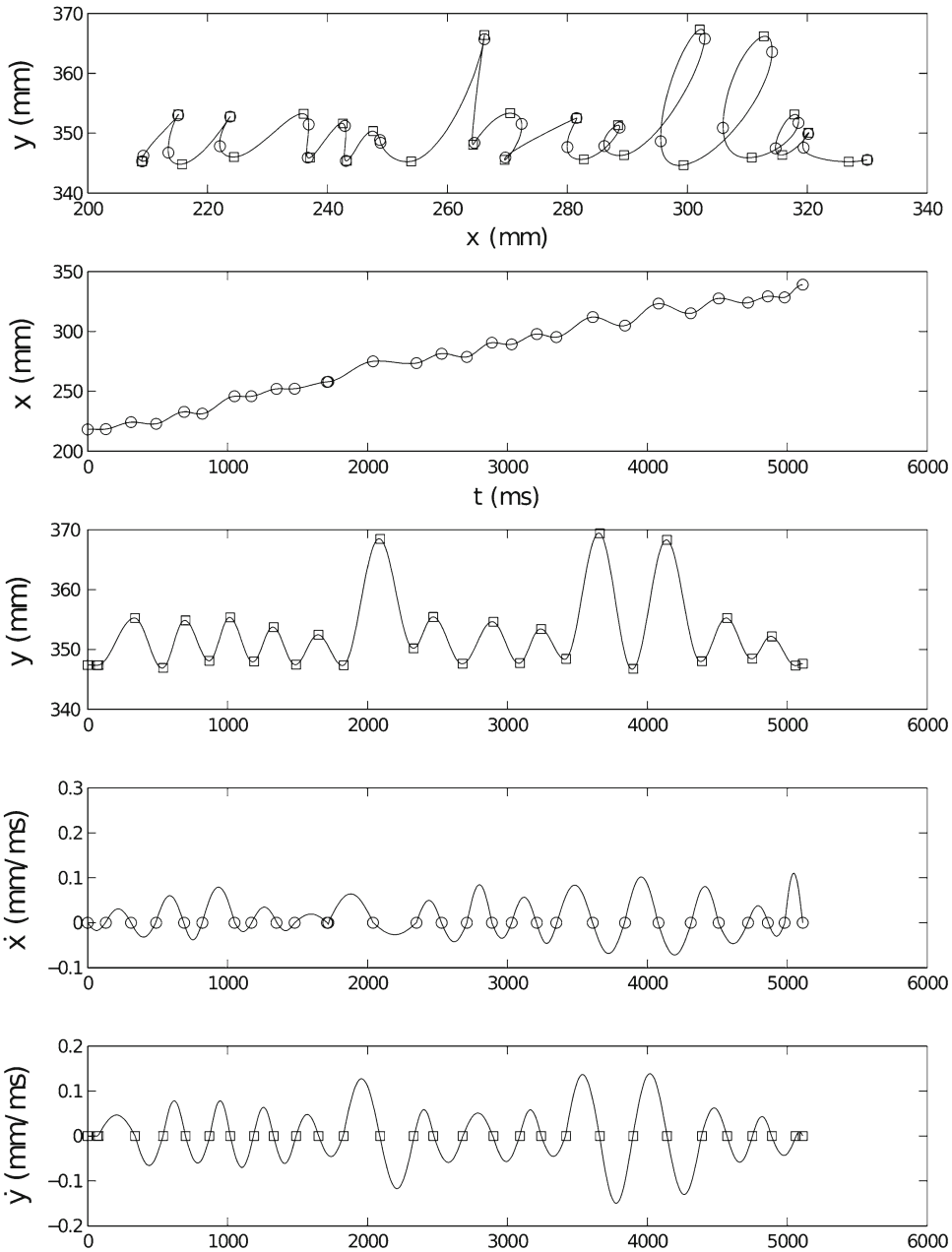

Fig. 2 The actual handwritten trace (*upper panel*), with the corresponding x and y position (*middle panels*) and velocity (*lower panels*) as a function of time. *Circles* (resp. *squares*) indicate the moments of x (resp. y) null velocity. Units (mm for positions, ms for time and mm/ms for velocities) are the same for all subsequent images)

$$t_{x,i+1} - t_{x,i} = \frac{\pi}{\omega_{x,i}} \quad \text{and} \quad \omega_{x,i} t_{x,i} + \phi_{x,i} = 0 \tag{22}$$

Hence formulas (7), (8) and (10), (11)

2.4.2 Computation of amplitude parameter a

Consider the following function:

$$f : x \mapsto a \sin(\omega x + \phi) \tag{23}$$

where a, ω and ϕ are independent of x. The mean and variance of between two successive zeros are:

$$M = \frac{\omega}{\pi} \int_{\frac{-\phi}{\omega}}^{\frac{\pi-\phi}{\omega}} f(x)\mathrm{d}x = \frac{2a}{\pi} \tag{24}$$

$$V = \frac{\omega}{\pi} \int_{\frac{-\phi}{\omega}}^{\frac{\pi-\phi}{\omega}} (f(x) - M)^2 \mathrm{d}x = \frac{a^2\left(-8+\pi^2\right)}{2\pi^2} \tag{25}$$

This shows that the amplitude of a sinusoidal signal can be approximated by the mean or the variance of this signal on a semi-period (zero to zero), independently of the frequency and phase, hence formulas in Eqs. (9) and (12).

2.4.3 Minimum number of parameters

Following Teulings (1996), it is interesting to assess the minimum number of parameters to be extracted from written trace and to be updated in the model to reconstruct a particular handwriting sample. Here, among the parameters of each oscillator [see Eqs. (19) and (20)], the ϕ and $t_{x/y}$ series are superfluous since they can be readily computed at reconstruction time from the following elements:

- The initial values $(t_{x,0}, a_{x,0}, \omega_{x,0}, \phi_{x,0})$ and $(t_{y,0}, a_{y,0}, \omega_{y,0}, \phi_{y,0})$
- The series $(a_{x,i}, \omega_{x,i})$, $1 \leq i < N_x$ and $(a_{y,i}, \omega_{y,i})$, $1 \leq i < N_y$

The model is fairly parsimonious, since it needs only the computing of two parameter values—the value of amplitude and value of frequency—for each update, every half period for x and y alternately. For instance, when writing a l letter (see Fig. 2 at about 4,000 ms), two parameter updates on the x-axis are required, as well as two updates on the y-axis, hence four updates. As a result, a total number of 8 value changes are necessary.

2.5 Parameter extraction algorithm for a sampled trace

Suppose that the recorded handwriting sample is represented by a chronological finite list of $\mathfrak{N}$ timestamped positions:

$$S = (t_i, x_i, y_i)_{1 \leq i \leq \mathfrak{N}, \mathfrak{N} \in \mathbb{N}^*, \forall i > 1, t_i > t_{i-1}} \tag{26}$$

Here follows an algorithm for extracting the series of parameters (19) and (20) from this recorded trace:

Step 1 $x = (x_i)_{1 \leq i \leq \mathfrak{N}}$ is differentiated according to $t = (t_i)_{1 \leq i \leq \mathfrak{N}}$:

$$\dot{x} = \left(\frac{x_i - x_{i-1}}{t_i - t_{i-1}} \right)_{1 < i \leq \mathfrak{N}} \tag{27}$$

$y = (y_i)_{1 \leq i \leq \mathfrak{N}}$ is differentiated according to $t = (t_i)_{1 \leq i \leq \mathfrak{N}}$:

$$\dot{y} = \left(\frac{y_i - y_{i-1}}{t_i - t_{i-1}} \right)_{1 < i \leq \mathfrak{N}} \tag{28}$$

Step 2 An extra zero velocity is added at the beginning and at the end of the velocity series on x and y. Otherwise, the forthcoming estimation of oscillatory parameters is impossible before the first zero crossing and after the last zero crossing. Indeed, oscillatory parameters can be estimated only between two successive zero crossings on each axis. This decision, although sometimes unrealistic, avoids additional computations.

Step 3 A zero crossing algorithm is applied to the derivatives, which have been low-pass filtered first (using a flat window of size 6). This filtering prevents the algorithm to find clusters of zeros due to acquisition irregularities or noise. This step yields the two series $t_{x,1}, \ldots, t_{x,N_x}$ and $t_{y,1}, \ldots, t_{y,N_y}$.

Step 4 The parameter series elements are computed:

$\forall i, 1 \leq i < N_x$:

$$\omega_{x,i} = \frac{\pi}{t_{x,i+1} - t_{x,i}} \tag{29}$$

$$\phi_{x,i} = -\frac{\pi t_{x,i}}{t_{x,i+1} - t_{x,i}} \tag{30}$$

$$a_{x,i} = \frac{\pi}{2} mean\,(\dot{x})_{[t_{x,i}, t_{x,i+1}[} \tag{31}$$

$\forall i, 1 \leq i < N_y$:

$$\omega_{y,i} = \frac{\pi}{t_{y,i+1} - t_{y,i}} \tag{32}$$

$$\phi_{y,i} = -\frac{\pi t_{y,i}}{t_{y,i+1} - t_{y,i}} \tag{33}$$

$$a_{y,i} = \frac{\pi}{2} mean\,(\dot{y})_{[t_{y,i}, t_{y,i+1}[} \tag{34}$$

Step 5 The x and y velocities are reconstructed, using Eqs. (5) and (6) and given the computed parameter series. The x and y traces are reconstructed by integration of these velocity values.

Figure 3 shows a sample trace superimposed with the trace reconstructed from the extracted parameters using the algorithm. Not only the reconstructed sentence is readable but also the individual properties of the letter formation are captured by POMH as well, even though the traces are quite complex, including abrupt changes in derivatives, corresponding to peculiar topological features of handwriting (e.g., spikes, reversal points, …).

Note that in Fig. 3, only the visible traces have been processed: The pen-lifted portions of the entire trajectory have been excluded from the analysis. Nonetheless, if these pen-lifted portions are processed, they are readily included in the analysis without any special treatment as can be seen in Fig. 12.

3 Comparison with Edelman–Flash model (EFM)

The efficacy of POMH parameter extraction and trace reconstruction can be assessed by comparison with those provided by another model. Unfortunately, Hollerbach's (1981) work, aiming to computer generation of handwriting-like traces, offered no method of parameter extraction from real, cursive

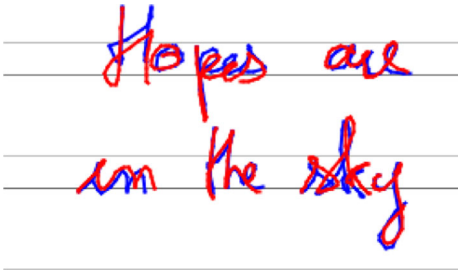

Fig. 3 Comparison of an actual handwritten (*blue line*) and POMH-reconstructed (*red line*) sentence (color figure online)

handwriting produced by humans. We compared our POMH model to the Edelman and Flash model (EFM, Edelman and Flash 1987; Edelman et al. 1990), already used elsewhere for comparison purposes (Paine et al. 2004). The interest of EFM undertaking lies in its completeness: The model was ultimately designed to reconstruct any real handwriting trace and Edelman and Flash proposed a quantitative method to assess its matching the real traces.

Using piecemeal generation approach, Edelman and Flash (1987) envisioned global handwriting trace as the concatenation of four prototypical strokes: a hook, a cup, an inversed gamma and an oval. The letter 'a,' for instance, was viewed as a concatenation of oval, cup and hook. The minimum jerk model is then applied to construct the trajectory from the relative positions of the start point, the via point, situated approximately in the middle of the planned trajectory and the end point of an actual stroke. EFM offered an excellent fit for the prototypical strokes as well as for letters, provided that, beforehand, the actual trace is separated into successive strokes. We expect that the matching between the real and the reconstructed profiles (position and velocity) with our model is at least as good as that achieved by the EFM model.

3.1 Methods

3.1.1 Participants

Four unpaid volunteers, three males and one female, aged between 24 and 49, took part in the study. Two participants were self-claimed right handed, two left handed. They reported normal or corrected-to normal visual acuity and had no physical impairment impeding detection and production of the required trace. The study was approved by the local ethical committee of Paul Sabatier Toulouse University, and participants provided a written informed consent in accordance with the Helsinki Declaration.

3.1.2 Material

The graphic task was performed on a computer-controlled graphic tablet (WACOM DTZ-1200W/G) with LCT screen of 261.1 × 163.2 mm size and 1280 × 800 resolution, inserted in a tablet (405.2 × 269.7 × 17 mm) which can be freely rotated just like a sheet of paper. A white sheet in landscape orientation, lined by blue lines spaced by 150 mm, was displayed on the screen. The stylus used was approximately the same size (174.8 mm long, with a diameter of 14.8 mm) and weight (17 g) as a normal ballpoint pen. Participants were seated in a height-adjustable chair, facing the graphic tablet set on a table, and asked to adopt the most comfortable writing posture. As soon as the stylus was less than 5 mm from the screen, the x and y spatial coordinates of the performed trajectories were digitized at 100 Hz with a spatial resolution announced at 0.005 mm. The produced trace was displayed in real time on the screen and its coordinates stored for further analysis. When the stylus raised 5 mm above the tablet, data recording stopped. This procedure allowed each required trace to be stored in a separate file.

3.1.3 Procedure

The set of required traces was composed of four prototypical strokes distinguished by Edelman and Flash (1987): a hook, a cup, a gamma and an oval, as discussed above. For each required stroke, participants were instructed to write 60 exemplars, using cursive handwriting at their spontaneous speed. Among the exemplars, the 20 middle exemplars were selected for analysis purposes. To collect handwritten traces in as natural a setting as possible, participants were not asked to rest the pen at the starting position prior to beginning to write. As a result, their hands were already in motion when the pen hit the writing surface. The whole experimental procedure lasted about 15 min.

3.1.4 Data analysis and reduction

Statistical analysis focused on the four prototypical strokes, for which both POMH and Edelman–Flash methods can be applied. In line with Edelman and Flash (1987), the matching between the produced and the reconstructed strokes was calculated through typical correlations on x-position, y-position, x-velocity and y-velocity. The classic Pearson-R formula was chosen here instead of that used by Edelman and Flash (1987) because the latter contains possible artefacts leading often to correlation values greater than 1. This correlation captures the topological similarity between the real and reconstructed stroke, without being affected by a possible vertical shift or change in amplitude between the real and reconstructed trace. The correlation index (R) varies from 1 for identical traces to -1 for mirror-inversed traces and tends toward zero when the matching deteriorates.

3.1.5 Minkowski p-dissimilarity

A global assessment of the (dis)similarity between EFM and POMH was captured using Minkowski p-dissimilarity metric. This metric captured the distance between the two models in a four-dimensional space, each dimension corresponding to one of the above correlation (R) between the real and the reconstructed stroke. For each participant, the EFM and POMH represent two points in the four-dimensional space, and Minkowski distance, d, corresponds to the vector joining them. Minkowski distance is a generalization of Euclidean distance:

$$d = \left(\sum_{i=1}^{p} |R_{\text{EFM}} - R_{\text{POMH}}|^p \right)^{\frac{1}{p}} \tag{35}$$

where p is the number of dimensions or the power for the norm of the vector. The Minkowski distance with power $p = 4$ was used here instead of the most often used power $p = 2$, in order to give a greater weight to the variables on which the models differ most. Minkowski distance equals 0 when the two methods are identical. Conversely, the largest distance between the best-matching model ($R = 1$) and the worst matching model ($R = 0$) amounts to:

$$d_{\max}(\text{EFM}, \text{POMH}) = \left(\sum_{i=1}^{4} |1 - 0|^4 \right)^{\frac{1}{4}} = 1.414 \tag{36}$$

3.1.6 Statistical analysis

Friedman ANOVA's, a nonparametric alternative to one-way repeated-measures analysis of variance, were used. Each dependent variable was analyzed separately using a 2 (Model = POMH, EFM) Friedman ANOVA to test whether there was a difference between the matching provided by POMH and EFM. An additional 4 (Stroke = oval, gamma, hook, cup) Friedman ANOVA carried out on the Minkowski distance aimed to assess whether the matching is distinct between closed (i.e., oval and gamma) and open (i.e., hook and cup) strokes.

3.2 Results

3.2.1 Visual inspection of individual data

Figures 4, 5, 6 and 7 provide individual samples of actual prototypical strokes, produced by humans: a hook (Fig. 4), a cup (Fig. 5), a vertically flipped gamma (Fig. 6) and an oval (Fig. 7). Each figure illustrates the produced stroke (upper panel), the time series of position (middle panels) and velocity (lower panels) on x and y (left and right panels, resp.).

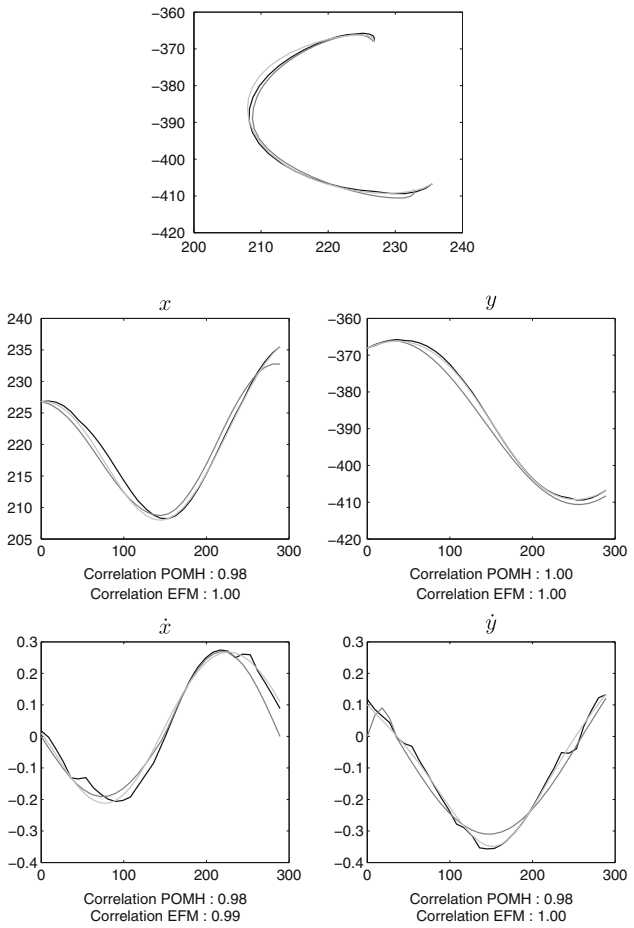

Fig. 4 Comparison between the actual (*black*), reconstructed by POMH (*dark gray*) and by EFM (*light gray*) traces for the 'hook' prototypical stroke, and the associated correlation indexes (see text for details)

Visual inspection of the graphic patterns (upper panels) suggests that both POMH (dark gray line) and EFM (light gray line) models fit the produced stroke (black line) quite well. Correlation indexes displayed below the panels are high for both models, all exceeding 0.97 value. Only trifling differences manifested at the second decimal arise between the fit produced by the POMH and EFM.

3.2.2 Correlation index

Correlation indexes are displayed in Table 1. For all prototypical strokes and all variables, the difference between POMH and EFM was lower than 0.1. Positive differences signal that POMH matched better the produced stroke than EFM. In Table 1, a star denotes a statistically significant difference ($p < 0.05$) between the two models.

A 2 (Model) Friedman ANOVA carried out on the oval prototypical stroke revealed that there was a statistically significant difference between the models for x-velocity, y-

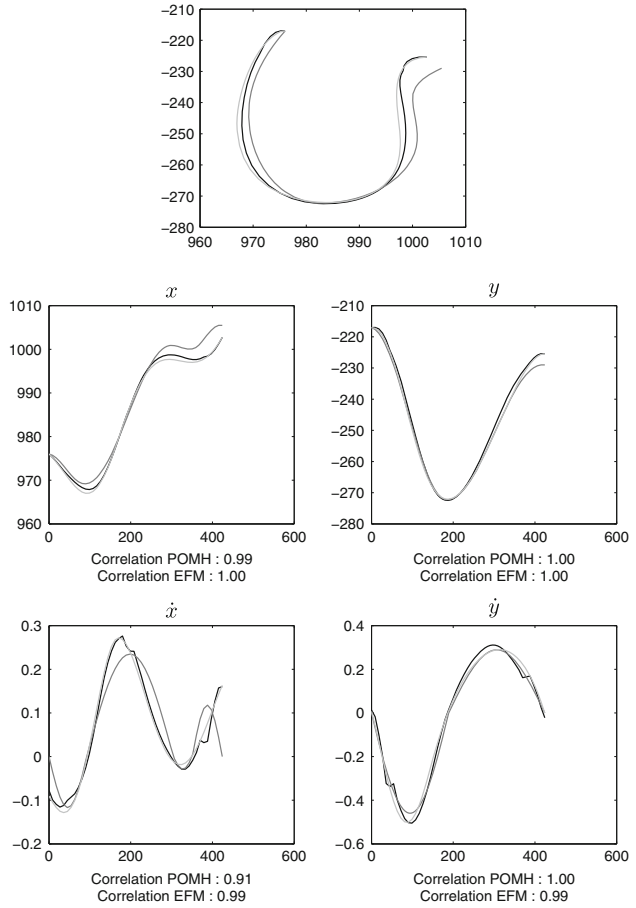

Fig. 5 Comparison between the actual (*black*), reconstructed by POMH (*dark gray*) and by EFM (*light gray*) traces for the 'cup' prototypical stroke, and the associated correlation indexes (see text for details)

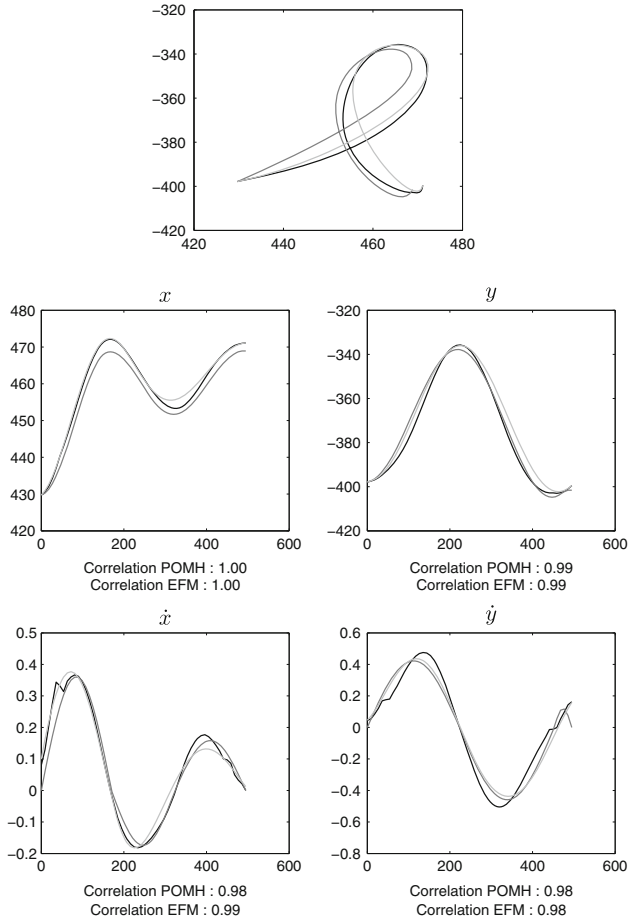

Fig. 6 Comparison between the actual (*black*), reconstructed by POMH (*dark gray*) and by EFM (*light gray*) traces for the 'gamma' prototypical stroke, and the associated correlation indexes (see text for details)

position and y-velocity. POMH model led to a higher correlation for the three variables.

A 2 (Model) Friedman ANOVA carried out on the gamma prototypical stroke revealed that there was a statistically reliable difference between the models for x-position, x-velocity, y-position and y-velocity. POMH model led to a larger correlation for the four variables.

A 2 (Model) Friedman ANOVA carried out on the hook prototypical stroke revealed that there was a statistically reliable difference between the models for x-position and y-velocity. EFM led to a higher correlation for the two variables.

A 2 (Model) Friedman ANOVA carried out on the cup prototypical stroke revealed that there was a statistically reliable difference between the models for x-position and y-velocity. EFM led to a higher correlation for the two variables.

3.2.3 Minkowski p-dissimilarity

Mean Minkovsky distance was 0.242 (SD = 0.022) for oval, 0.298 (SD = 0.065) for gamma, 0.151 (SD = 0.063) for hook and 0.228 (SD = 0.041) for the cup, which is much smaller than the maximum Minkowski distance of 1.414 (see Eq. 36). For oval and gamma where there is a large discrepancy between the two models in terms of Minkowski distance, correlations shows that POMH performs a better matching (see differences for oval and gamma in Table 1). However, a 4 (Stroke) Friedman ANOVA carried out on p-dissimilarities between all prototypical strokes revealed no significant effect ($p > 0.05$). Overall, the above results indicate that the matching for POMH and EFM was similar for all strokes.

3.2.4 Samples of roman handwritten traces

Beyond the reconstruction of basic prototypical strokes, POMH makes it possible to simulate longer pieces of handwriting, such as letters ('b' and 'h,' Figs. 8, 9), words ('lune,' Fig. 10), signatures (Fig. 11) and sentences ('la mort du jeune radis,' Fig. 12). Correlation indexes for the more complete

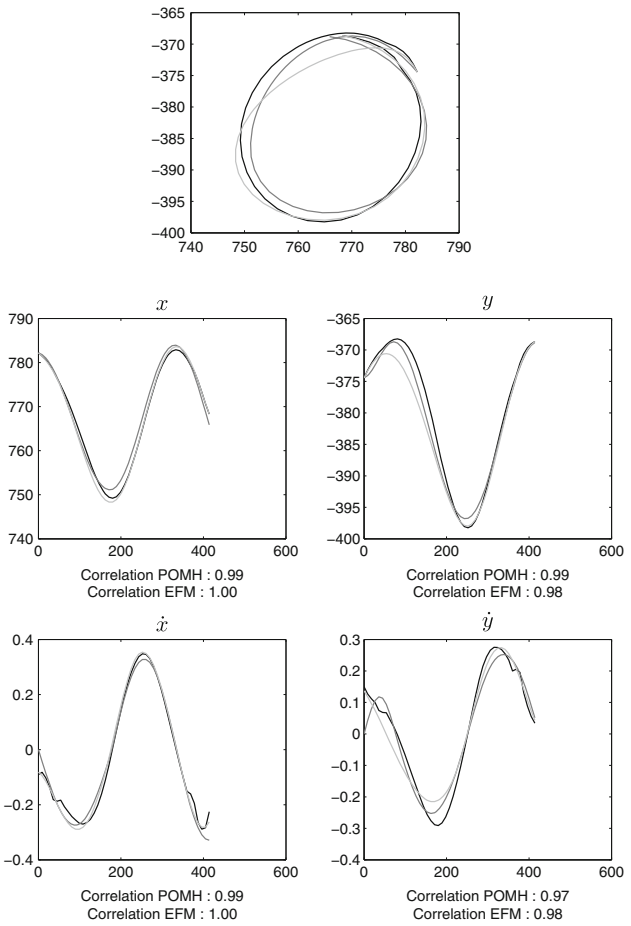

Fig. 7 Comparison between the actual (*black*), reconstructed by POMH (*dark gray*) and by EFM (*light gray*) traces for the 'oval' prototypical stroke, and the associated correlation indexes (see text for details)

and natural handwriting samples are in the range of those for the shorter prototypes studied above (i.e., 0.9). Notably, POMH is successful in reconstructing signatures, which often escape the school-imposed well-behaved forms and lead to idiosyncratic patterns. Notably, these free-running traces are quite a challenge for prototype-based models.

3.2.5 Samples of non-roman handwritten traces

In order to assess how good the POMH model is to handle handwriting systems that bear on the production of discrete movements such as Japanese kanji or Chinese ideograms, we asked a Chinese subject to write the Chinese word for 'table' at her most natural speed on our experimental writing tablet. The pen movement was recorded when it was on the sheet ($z = 0$; writing) and above the sheet ($z > 0$; flying between two strokes). The trace was analyzed through the POMH parameter extraction algorithm and reconstructed. The results are displayed on Fig. 13.

Figure 13 top-left shows the produced movement trajectory on and above the sheet ($z \geqslant 0$) and top-right shows its reconstruction by POMH; Fig. 13 middle-left shows the movements on the sheet only ($z = 0$) and middle-right its reconstruction by POMH. The last row shows the corresponding speed profiles for x and y.

The trace reconstructed by POMH, with its dynamics, is good, with a high degree of correlation between the actual and reconstructed velocities on both dimensions. Interestingly, both velocity profiles exhibit rhythmic fluctuations, very similar to those observed for continuous handwriting with Latin characters, words and sentences (cf. Fig. 2 for instance). Although the trace in Chinese writing is obviously discrete, the underlying generative process remains of a periodic nature.

The preliminary results, which certainly need to be confirmed with a larger data set, indicate that when the complete motion of the pen is considered, on and above the sheet, which avoids separating the successive strokes from each other, 'discrete' writing systems might well be described in terms of coordinated oscillatory motion, as it is the case for 'continuous' handwriting.

4 Discussion

Elaborating on the original Hollerbach's work (1981), our aim was to provide a model of handwriting production and, more generally, of 2D trace generation. The task was two-pronged: determining when and how the model parameters are extracted and updated and making the model general enough to account for a large diversity of handwritten traces. The core of our contribution lies in the symmetry of the equations and in an autonomous algorithm for extracting the model parameters. This leads to a reconstruction of handwritten traces without resorting to complex procedures of optimization and of prototypes identification. The computation of amplitude, in particular, benefited from a new mathematical result based on the sum of the mean value and the standard deviation over the last semi-period. We discuss below the mathematical features of our model, its performance in reconstructing an actual handwritten trace, its biological plausibility and future directions for development.

4.1 A parsimonious model of cursive handwriting

For the x and y movements to be truly oscillatory, their parameters should not change in a continuous way (otherwise, the choice of an harmonic driving function would be somewhat arbitrary), and even not too often (otherwise, it would be an ad hoc mapping of the trace with small arcs of ellipses, a piecemeal operation). By virtue of this oscillatory premise, the trajectory between two zero crossings in the velocity pro-

Table 1 Mean and standard deviation (SD) of correlation indexes for the four mentioned dependent variables for POMH and EFM, and results of subsequent ANOVA

	POMH	Edelman–Flash	Difference	Friedman ANOVA
	Mean (SD)		Mean	p
Oval				
x	0.97 (0.02)	0.93 (0.08)	0.04	0.31
$\dot{x}$	0.96 (0.01)	0.88 (0.06)	0.08	0.05*
y	0.99 (0.00)	0.91 (0.07)	0.08	0.05*
$\dot{y}$	0.94 (0.01)	0.88 (0.07)	0.06	0.05*
Gamma				
x	0.99 (0.001)	0.93 (0.08)	0.06	0.05*
$\dot{x}$	0.95 (0.006)	0.88 (0.05)	0.07	0.05*
y	0.98 (0.002)	0.89 (0.10)	0.09	0.05*
$\dot{y}$	0.96 (0.005)	0.82 (0.10)	0.14	0.05*
Hook				
x	0.90 (0.13)	0.91 (0.13)	−0.01	0.05*
$\dot{x}$	0.90 (0.09)	0.89 (0.05)	0.01	1.00
y	0.94 (0.05)	0.92 (0.08)	0.02	0.37
$\dot{y}$	0.82 (0.12)	0.84 (0.10)	−0.02	0.05*
Cup				
x	0.81 (0.28)	0.85 (0.17)	−0.04	1.00
$\dot{x}$	0.88 (0.13)	0.91 (0.09)	−0.03	0.05*
y	0.91 (0.10)	0.95 (0.06)	−0.04	0.31
$\dot{y}$	0.79 (0.14)	0.87 (0.09)	−0.08	0.05*

* A statistically different value ($p < 0.05$)

files specified using two parameters only. The simplicity of this method made it possible to extract the parameters 'in real time' with any ordinary personal computer and pen tablet.

POMH parsimony mostly owes to its symmetry. In contrast to Hollerbach (1981) who implemented a method to update parameters for both x and y oscillators exclusively when velocity reached zero on the y axis, we posited the parameters to be changed at the velocity zero crossings for each x and y oscillators separately. Thus, symmetry is preserved since the axes or the oscillators can be swapped. From there, a unique and simple algorithm, based on elementary trigonometric operations, could be applied for reconstructing the velocity profiles of both oscillators motion. Hollerbach (1981) took another track: By using zero crossings on the y axis only, the reconstruction of parameters on the x axis would call for additional, complex nonlinear methods of fitting.

As a first consequence, symmetry allows obviating a specific account for the positional drift that occurs along the x-axis during writing. Whereas Hollerbach (1981) or Singer and Tishby (1994) abstracted and implemented the drift separately, POMH accounts for the right-to-left displacement by the mere generation of the oscillations on the x axis, provided that the phase accumulates across cycles. Actually, the procedure could work as efficiently, irrespective of the leading direction of the handwriting (right-to-left, top-to-bottom). In contrast to Singer and Tishby (1994), no assumption was formulated about the phase, amplitude or frequency values at the moment of their updating. Singer and Tishby (1994) stipulated that when velocity reaches zero, a null phase should be reset on y and the same frequency is attributed to both x and y.

As a second consequence, symmetry endowed POMH with the possibility of information transfer across successive updates, some kind of partial memory of the trace that has just been written. For instance, while parameters are being extracted from x-trajectory at a given update, the model keeps using the parameters that had been just extracted from y-trajectory, and vice-versa. As a result, the trace is not produced in a serial, piecemeal manner: The newly extracted parameters to be implemented for one dimension of the ongoing trace are intermixed with those inherited from the previous update for the other dimension. Such an 'information transfer' on a quarter of a cycle basis is likely to account for the smoothness of the reconstructed traces.

Finally, symmetry made also our model insensitive to x and y swapping; Actually, there is no need for any a priori fixed spatial coordinate system. In the present case, we decided to set the x and y axes orthogonally in reference to the paper sheet (i.e., the tablet), but the model could work with any other spatial reference. This property can be used for practical purposes: When there are long straight segments

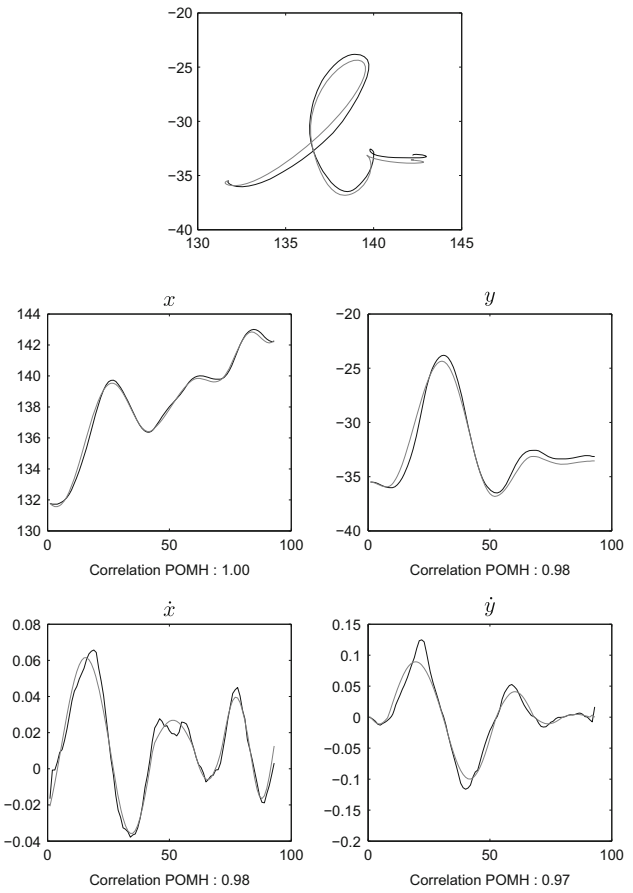

Fig. 8 Comparison between the actual (*black*) and reconstructed by POMH (*gray*) traces for the 'b' letter, and the associated correlation indexes (see text for details)

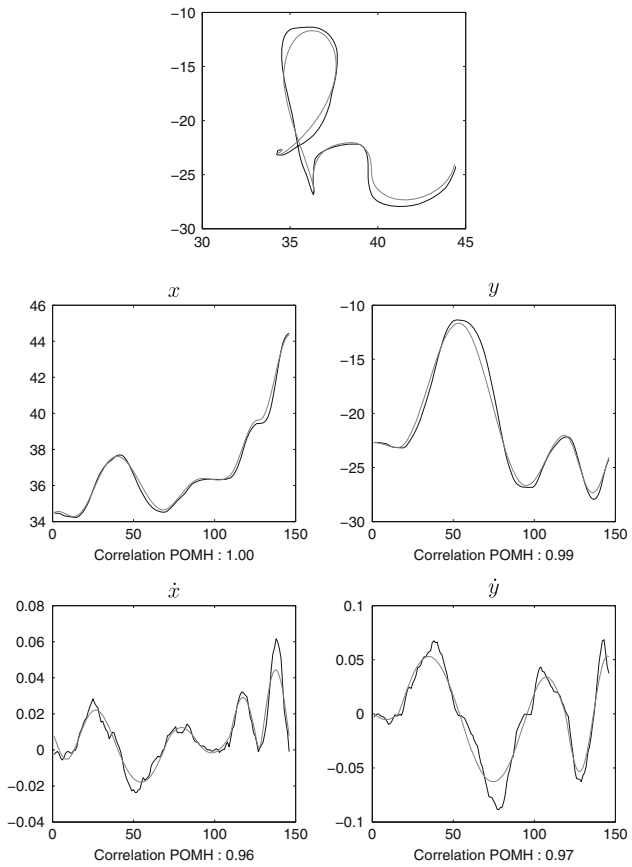

Fig. 9 Comparison between the actual (*black*) and reconstructed by POMH (*gray*) traces for the 'h' letter, and the associated correlation indexes (see text for details)

along an axis, which entails a bad detection of zero crossings, POMH turns out to work better with a rotated and/or non-orthogonal coordinate system.

On the whole, the POMH model emphasizes a well-known lesson in dynamical systems: Complex behavior, here handwritten traces, can be generated using an astonishingly simple algorithm; sophisticated outputs do not require heavy and arcane computations. Here, feature properties of motor behavior, such as smoothness of trajectory or independence from a coordinate system, can arise 'for free' from the interaction of simple, generative operations, without being specifically and intentionally specified and implemented.

4.2 Trace topology and movement dynamics

In order to evaluate the performance of POMH, we compared it to a well established, yet very different handwriting model by Edelman and Flash (1987). Using the handwriting prototypes proposed by these authors, our statistical results suggest that POMH matched the traces produced by humans equally well as Edelman and Flash's method, which involves a much more complex optimization algorithm. Our results were drawn from the raw acquisition data, in particular without smoothing, contrary to Edelman and Flash. POMH is able to deal with all the diversity of cursive handwriting topology (loops, reversal points, crossings, inclusions) which can be fully but simply and directly described by inversions of relative phase and changes in amplitude. Moreover, the POMH model presents the additional feature of exactly reproducing the kinematics of the movement: The superposition of the trajectory is not only spatial, but spatiotemporal, so that the actual and reconstructed traces unfold similarly in 'real time.' This suggests that the dynamical features of human motion, in the instance of handwriting here, are properly reproduced by the model and may stem from the very combination of the oscillatory motion in the two spatial dimensions (Lacquaniti et al. 1983).

POMH presents an acceptable balance between the accuracy of the matching and the number of parameters used to obtain the result. Theoretically and pragmatically, it does not always make good sense to distort the reconstructed trace in order to fit all the variations in the trace actually produced (Burnham and Anderson 2002). Some of the variations rep-

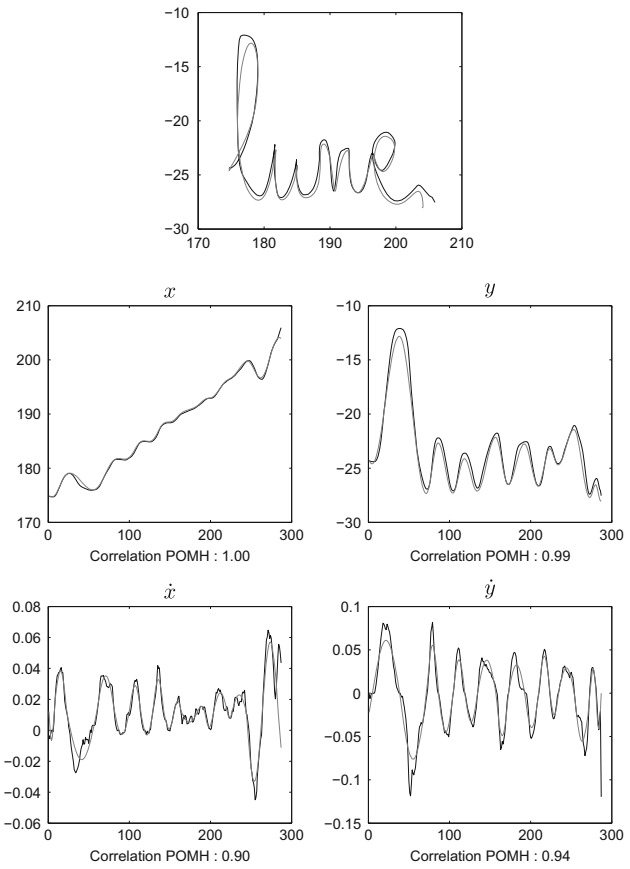

Fig. 10 Comparison between the actual (*black*) and reconstructed by POMH (*gray*) traces for the 'lune' word, and the associated correlation indexes (see text for details)

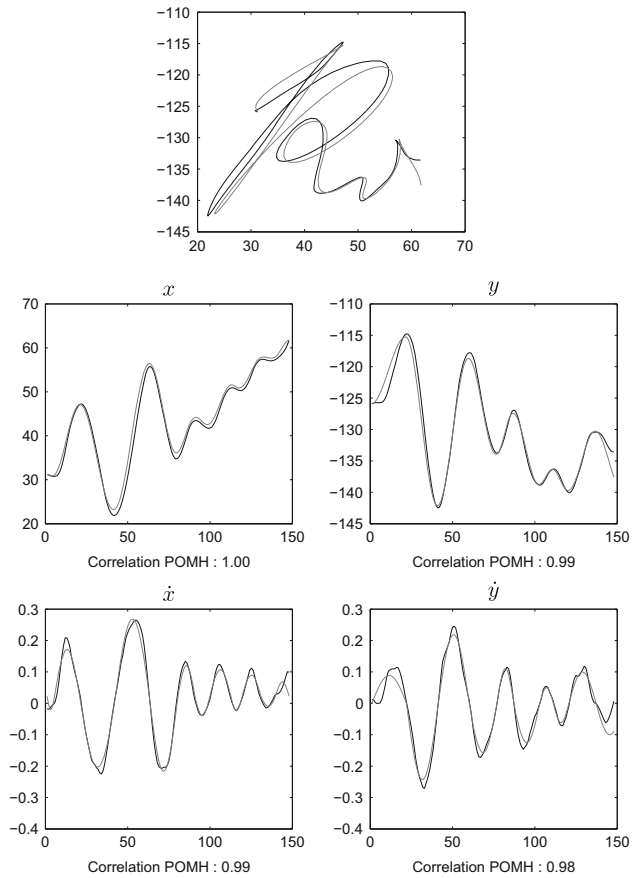

Fig. 11 Comparison between the actual (*black*) and reconstructed by POMH (*gray*) traces for an individual signature, and the associated correlation indexes (see text for details)

resent only noise, without any informative value on the data structure (Pitt and Myung 2002). Besides the above problem of overfitting, it must be kept in mind that human (motor) behavior is flawed with an irreducible variability: A trajectory is never reproduced in an identical manner. It can then be argued that the accuracy in reconstructing a trajectory by a mathematical model does not have to exceed the possibility of an accurate production of the trajectory by a human. Our results appear to be quite within the variability expected from a human writer.

4.3 Biological plausibility

Besides its compactness, parsimony and efficiency, a fourth feature of POMH is its biological plausibility. The assumption of the basically oscillatory motion adopted here is in agreement with the frequency spectrum of the pen-tip movements observed in the Cartesian space (Dooijes 1983; Kunesch et al. 1989). Moreover, despite its specificities, handwriting obeys the same generic laws as other non-discrete, cyclic movements, whose dynamics are successfully captured by oscillatory models (Athènes et al. 2004).

In addition, POMH exhibits two other realistic properties of human handwriting. First, by extracting parameters independently on the x and y dimensions, so that all parameters are never renewed at the same time, the model evacuates one of most documented problematic issue in biological movement generation: coarticulation. This notion reflects the fact that the kinematics of an ongoing stroke is influenced by that of the previously traced one (Thomassen and Schomaker 1986). Second, POMH being free of a specific spatial coordinate system entails another prominent property of human movement: motor equivalence (Lashley 1942; Teulings 1996; Wing 2000). Motor equivalence is the faculty to achieve the same output through any combination of motor configurations. The redundancy of the motor system that permits motor equivalence forbids a strict mapping between the mobilized effector and the reference system. Thus, humans can change the orientation of the paper sheet and vary their penhold while writing (Sassoon 1993) or they can trace the same graphic pattern using the shoulder, the elbow, the wrist or the fingers, or even the foot, the neck or the teeth (Bernstein 1935).

The property of motor equivalence suggests that the graphic motion is specified by the CNS at a more abstract

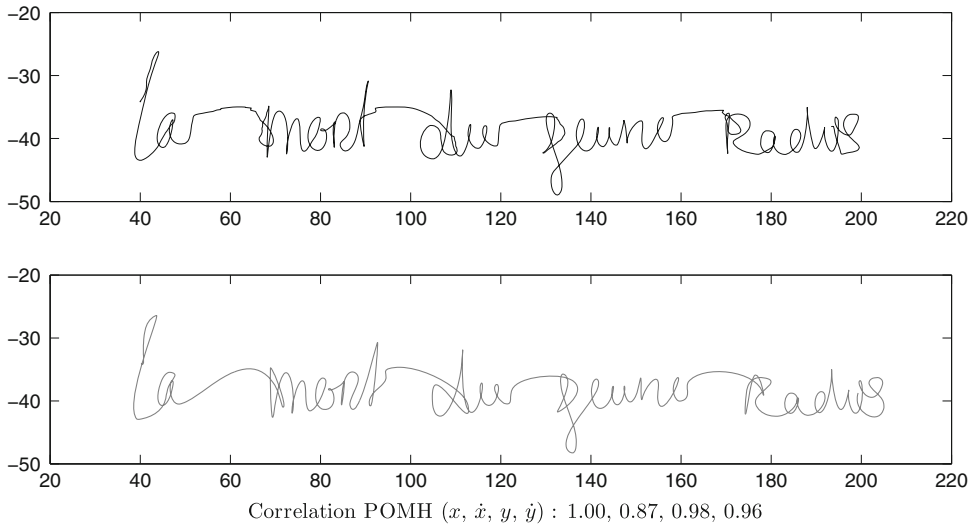

Fig. 12 Comparison between the actual (*top panel*) and reconstructed by POMH (*bottom panel*) traces for the 'la mort du jeune radis' sentence, and the associated correlation indexes (see text for details)

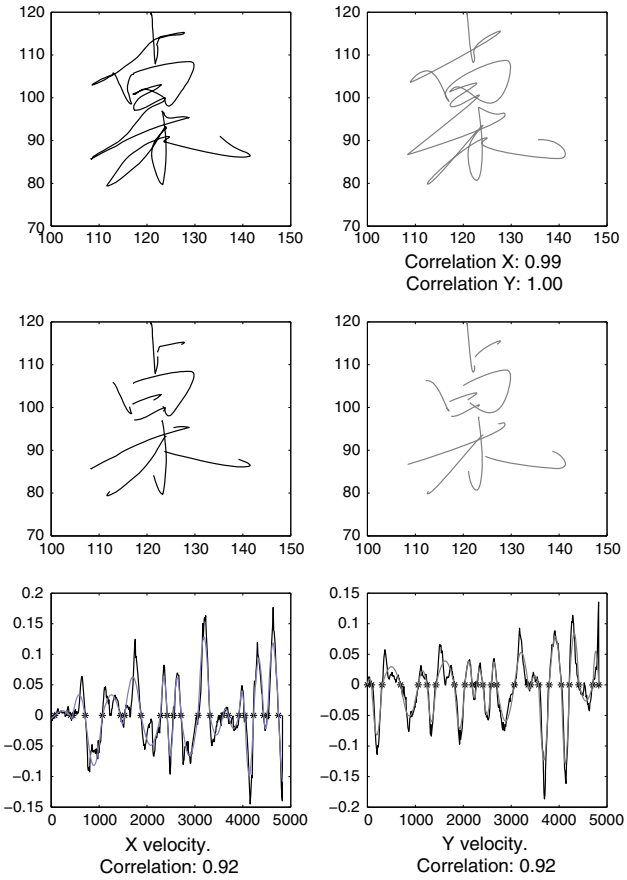

Fig. 13 Comparison between the actual (*black*) and reconstructed by POMH (*gray*) traces and velocities of a Chinese character and the associated correlation indexes (see text for details)

level than the actual specifications of the motor coordinates. With POMH, the graphic traces are reconstructed by providing particular phase, amplitude and frequency values. These are general properties of the oscillatory motion, which do no convey explicit information for their motor implementation. It must be emphasized that motor equivalence manifests itself only when the produced trajectories are long or complicated enough to exhibit specific topological features (such as branching or crossing). Thus, it is crucial that POMH succeeded in the reconstruction of long traces, such as real words and sentences, in addition to individual simple strokes and prototypes. Models accounting for short trajectories only cannot capture, by definition and in fact, motor equivalence.

The various traces that handwriting requires ask for mechanisms able to generate both continuous and discrete movements (Guiard 1993, 1997). Accordingly, on the level of motor outcome, trigonometric functions confer to POMH the possibility of producing both non-harmonic traces, containing full stops or reversal points, and more harmonic squiggles (see Fig. 3). On the level of processing, POMH instantiates an ongoing generative mechanism, endowed with intermittently updated parameters. Therefore, continuous trajectories are not envisioned here as the concatenation of discrete movements, but as the outcome of a specific mode of movement generation, an idea that is now supported by converging empirical evidence based on kinetic, kinematic, topological and neural features of discrete and continuous movements (Buchanan et al. 2006; Guiard 1993; Huys et al. 2008; Jirsa and Kelso 2005; van Mourik and Beek 2004; Perdikis et al. 2011).

If continuous movements resulted from the concatenation of discrete movements (aka strokes), discrete movements would involve less processing and would be more robust to disruption than continuous movement. Yet, neurobiological studies contradict this contention. Using fMRI, Schall et al. (2004) documented that in addition to primary motor areas activated for continuous movement, discrete movements recruit a variety of other brain regions, including cerebellum. Moreover, Spencer et al. (2003) showed that patients with cerebellar lesions have deficits in producing dis-

continuous but not continuous movements. Instead of being envisioned as basic building blocks, discrete movements can rather be conceived of as a limit case of oscillatory motion, that is, an aborted cyclic movement (Schöner 1990), or as a qualitatively distinct category of motion altogether irreducible to continuous motion (Jirsa and Kelso 2005).

Extracting parameters when velocity reaches a zero value is also behaviorally pertinent. Studies on human oscillatory motion (Beek 1989; Byblow et al. 1994) have shown that within each movement cycle, there are two specific, so-called anchor points, localized about movement reversals (viz. velocity amounts to zero). At these points, a local tightening of the trajectories in phase space reflects the availability of information instrumental to organizing the whole movement cycle, in particular to establish its temporal stability, as shown in studies on bimanual coordination (Fink et al. 2000). Kostrubiec et al. (2011) documented that bimanual patterns that were new to an individual and at first difficult to produce were nonetheless facilitated once the effectors were put into the right position at these very anchoring points. These findings suggest that the characteristics of the global movement cycle are chiefly defined at the local points where velocity is null.

4.4 Implications and future directions

A reason for the parsimony and efficiency of the POMH model stems from merging the steps of parameter extraction and movement generation into one single nonstop process. This view is quite in line with theoretical claims, frequent in the neurosciences and psychology, that in the human brain too, perceptual (viz. parameter extraction) and motor (viz. movement generation) processes are tightly related (e.g., Fowler and Turvey 1978; Gibson 1977; Kelso 1995). Strong empirical evidence is accumulating, first in the field of speech science in the fifties (e.g., Liberman and Mattingly 1985, for a review) that perception is strongly rooted into action, a basic tenet of so-called motor theories of perception (e.g., Galantucci et al. 2006, for a review). Many behavioral and, more recently, neurobiological findings indicate that such is the case for handwriting too, which turns out to be concurrent with reading (e.g., Nakamura et al. 2012). In the wake of the discovery of the 'mirror neurons' (Rizzolatti and Graighero 2004), studies using fMRI have shown that reading handwritten letters involved areas in the prefrontal cortex that are common with the network activated in reading the same letters, whereas this was not the case for printed letters or scribbles (Longcamp et al. 2003a). A finer analysis using ERP (Event-Related Potential) demonstrated that the involvement of the motor cortex in the discrimination of letters is fairly precocious, as early as 300 ms after the stimulus (Wamain et al. 2012), this effect being specific to self-produced handwritten letters, as compared to letters produced by another human or to a printed letter.

Of particular interest for the POMH model, which is, recall, rooted on oscillation, is the specific task of discriminating between ellipses of various eccentricities, shapes that are an outcome of the combination of two orthogonal oscillators (aka Lissajou plots). A recent study using a dual-task paradigm evidenced that a concurrent motor task (successive multi-finger tapping) interferes with visual perception exclusively for ellipses that are actually produced in the most stable and precise fashion (Wamain et al. 2011). Thus, the motor areas subserving the movement of the hand are significantly more involved in the detection and discrimination of shapes that correspond to stable motor patterns, as compared to shapes corresponding to less stable ones. And this holds true on an individual basis: What each writer has eventually grown to prefer to perform as a graphic output is also what s/he tends to discriminate best and fastest. This may be a basic mechanism through which children learn to write and read concomitantly (Longcamp et al. 2003b), while the basic repertoire of coordinated oscillatory patterns of adults (Athènes et al. 2004) is progressively acquired during childhood (Danna et al. 2012).

A second reason for parsimony and efficiency is that our model intermittently updates the relevant parameters of a continuously outputted function, so that traces of increased complexity can be successfully reconstructed, going from simple strokes to words, sentences and signatures.

Still, the very process of intermittent updating of an oscillation raises several issues. The first issue pertains to the assumption of a stable frequency. For instance, in their model (see above), Singer and Tishby (1994) reset the phase to zero every half-cycle and accounted for the variations in the produced shape by changes in frequency. Notwithstanding, experimental observations suggest the contrary: Frequency tends to be stable, while phase varies. In a series of experiments, Viviani and Terzuolo (1980) demonstrated that, when drawing circles of varying size alternately, movement velocity varied proportionally to the length of the produced trajectory, so that movement time was maintained fairly constant. This principle of isochrony, also found in reaching and pointing movements without time or precision constraints (described for example by Gordon et al. 1994), presupposes that fairly natural movements tend to maintain movement time, hence frequency, constant. If handwriting follows the rule of isochrony, then the POMH model is right in assuming a stable frequency and a variable phase.

Another issue pertains to the updating process. In the POMH model, the parameters are specified for each axis every half-cycle alternately, leading to a mechanism running on a quarter of a cycle basis. Obviously, daily life experience as well as numerous experimental findings concur to indicate that longer bouts of trajectory can be produced without

update. Further work is underway to find out whether successive quarters of a cycle can be merged into larger chunks with similar parameters.

The take-home message of the present study is that a complex motor skill, such as handwriting, can be still simulated by a simple model, provided that the basic dynamic property of the movement, namely, its oscillatory nature, is at the heart of the model. As a result, our POMH model is able to capture parameters from real handwritten traces and reconstruct them accurately in space and time. This may be an valid instance of a computer-biological platform (Prinz et al. 2004), where the actual parameters and the simulated outcome are matched in order to perform a severe and robust test of the model.

References

Athènes S, Sallagoïty I, Zanone PG, Albaret JM (2004) Evaluating the coordination dynamics of handwriting. Hum Mov Sci 23:621–641

Beek PJ (1989) Juggling dynamics. PhD thesis. Free University Press, Amsterdam

Bernstein N (1935) The problem of the interrelation of co-ordination and localization. Arch Biol Sci 38:15–59

Blöte AW, Zielstra EM, Zoetewey MW (1987) Writing posture and writing movement in kindergarten. J Hum Mov Stud 13:323–341

Buchanan JJ, Park JH, Shea CH (2006) Target width scaling in repetitive aiming task: switching between cyclical and discrete units of action. Exp Brain Res 175(4):710–725

Bullock D, Grossberg S, Mannes C (1993) A neural network model for cursive script production. Biol Cybern 70:15–28

Burnham KP, Anderson DR (2002) Model selection and multi-model inference: a practical information-theoretic approach, 2nd edn. Springer, New York

Byblow WD, Carson RG, Goodman D (1994) Expressions of asymmetries and anchoring in bimanual coordination. Hum Mov Sci 13:3–28

Danna J, Enderli F, Athènes S, Zanone PG (2012) Motor coordination dynamicsunderlying graphic motion in 7 tp 11 year-old children. J Exp Child Psychol 111(1):37–51

Dooijes EH (1983) Analysis of handwriting movements. Acta Psychol 54:99–114

Edelman S, Flash T (1987) A model of handwriting. Biol Cybern 57:25–36

Edelman S, Flash T, Ullman S (1990) Reading cursive handwriting by alignment of letter prototypes. Int J Comput Vis 5:303–331

Ellis AW (1982) Spelling and writing (and reading and speaking). In: Ellis AW (ed) Normality and pathology in cognitive functions. Academic Press, London, pp 113–146

Fink P, Foo P, Jirsa VK, Kelso JAS (2000) Local and global stabilization of coordination by sensory information. Exp Brain Res 134:9–20

Fowler CA, Turvey MT (1978) Skill acquisition: an event approach with special reference to searching for the optimum of a function of several variables. In: Stelmach GE (ed) Information processing in motor control and learning. Academic Press, New York, pp 1–40

Galantucci B, Fowler CA, Turvey MT (2006) The motor theory of speech perception reviewed. Psychon Bull Rev 13(3):1–36

Gibson JJ (1977) The theory of affordances. In: Shaw RE, Bransford J (eds) Perceiving, acting, and knowing. Lawrence Erlbaum, Hillsdale, pp 67–82

Gordon J, Ghilardi MF, Ghez C (1994) Accuracy of planar reaching movements. I. Independence of direction and extend variability. Exp Brain Res 99(1):97–111

Guiard Y (1993) On Fitts' and Hooke's laws: simple harmonic movement in upper-limb cyclical aiming. Acta Psychol 82:139–159

Guiard Y (1997) Fitts' law in the discrete vs. continuous paradigm. Hum Mov Sci 17:97–131

Hollerbach JM (1981) An oscillation theory of handwriting. Biol Cybern 39:139–156

Huys R, Studenka BE, Rheaume NL, Zelaznik HL, Jirsa VK (2008) Distinct timing mechanisms produce discrete and continuous movements. PLoS Comput Biol 4(4):e100061

Jirsa VK, Kelso JAS (2005) The excitator as a minimal model for the coordination dynamics of discrete and rhythmic movements. J Mot Behav 37:35–51

Kandel S, Spinelli E (2010) Processing complex graphemes in handwriting production. Mem Cogn 38:762–770

Kelso JAS (1984) Phase transitions and critical behavior in human bimanual coordination. Am J Physiol Regul Integr Comp Physiol 15:1000–1004

Kelso JAS (1995) Dynamic patterns: the self-organization of brain and behavior. MIT Press, Cambridge

Kostrubiec V, Soppelsa R, Albaret JM, Zanone PG (2011) Facilitation of non-preferred coordination patterns during the transition from discrete to continuous movements. Mot. Control 15:456–480

Kunesch E, Binkofski F, Freund HJ (1989) Invariant temporal characteristics of manipulative hand movements. Exp Brain Res 78:539–546

Lacquaniti F, Terzuolo C, Viviani P (1983) The law relating the kinematic and figural aspects of drawing movements. Acta Psychol 54(1):115–130

Lashley KS (1942) An examination of the "continuity theory" as applied to discriminative learning. J Gen Psychol 26(2):241–265

Liberman AM, Mattingly IG (1985) The motor theory of speech perception revised. Cognition 21(1):1–36

Longcamp M, Anton JL, Roth M, Velay JL (2003) Visual presentation of single letters activates a premotor area involved in writing. Neuroimage 1:1492–1500

Longcamp M, Zerbato-Poudou MT, Velay JL (2003) The influence of writing practice on letter recognition in preschool children: a comparison between handwriting and typing. Acta Psychol 119:67–69

Meulenbroek RGJ, Van Galen GP (1989) The production of connecting strokes in cursive handwriting: developing co-articulation in 8 to 12 year-old children. In: Plamondon R, Suen CY, Simner ML (eds) Computer recognition and human production of handwriting. World Scientific, Singapore, pp 273–386

Nakamura K, Kuo WJ, Pegado F, Cohen L, Tzeng O, Dehaene S (2012) Universal brain systems for recognizing word shapes and handwriting gesture during reading. Proc Natl Acad Sci 109(20):20762–20767

Paine RW, Grossberg S, Van Gemmert AWA (2004) A quantitative evaluation of the AVITEWRITE model of handwriting learning. Hum Mov Sci 23(6):837–860

Patterson KE, Wing AM (1989) Processes in handwriting: a case for case. Cogn Neuropsychol 6:3–23

Perdikis D, Huys R, Jirsa VK (2011) Complex processes form dynamical architectures with time-scale hierarchy. PLoS One 6:e16589

Pitt MA, Myung IJ (2002) When a good fit can be bad. Trends Cogn Sci 6:421–425

Plamondon R, Djioua M (2006) A multi-level representation paradigm for handwriting stroke generation. Hum Mov Sci 25:586–607

Prinz AA, Abott LF, Marder E (2004) The dynamic clamp comes of age. Trends Neurosci 27:218–224

Rizzolatti G, Graighero L (2004) The mirror-neuron system. Annu Rev Neurosci 27:169–192

Sassoon R (1993) The art and science of handwriting. Intellect Ltd, Oxford

Sallagoïty I, Athènes S, Zanone PG, Albaret JM (2004) Stability of coordination patterns in handwriting: effects of speed and hand. Mot Control 8(4):405–421

Schall S, Stenard D, Osu R, Kawato M (2004) Rhythmic arm movement is not discrete. Nat Neurosci 7:1138–1143

Schöner G, Kelso JAS (1988) A synergetic theory of environmentally-specified and learned patterns of movement coordination. Biol Cybern 58:71–80

Schöner G (1990) A dynamic theory of coordination of discrete movement. Biol Cybern 63:257–270

Singer Y, Tishby N (1994) Dynamical encoding of cursive handwriting. Biol Cybern 71:227–237

Spencer RMC, Zelaznik HN, Diedrichsen J, Ivry RB (2003) Disrupted timing of discontinuous but not continuous movements by cerebellar lesions. Science 300:1437–1439

Stark L (1968) Neurological control systems. Studies in bioengineering. Plenum, New York

Teulings HL, Mullins PA, Stelmach GE (1986) The elementary units of programming in handwriting. In: Kao HSR, Van Galen GP, Hoosain R (eds) Graphonomics: contemporary research in handwriting. North-Holland, Amsterdam, pp 21–32

Teulings HL (1996) Handwriting movement control. In: Keele SW, Heuer H (eds) Handbook of perception and action, vol 2: Motor skills. Academic Press, London, pp 561–613

Thomassen AJWM, Schomaker LRB (1986) Between-letter context effects in handwriting trajectories. In: Kao HSR, Van Galen GP, Hoosain R (eds) Graphonomics: contemporary research in handwriting. North-Holland, Amsterdam, pp 253–272

van Mourik AM, Beek PJ (2004) Discrete and cyclical movements: unified dynamics or separate control? Acta Psychol 117:121–138

Viviani P, Terzuolo CA (1980) Space-time invariance in learned motor skills. In: Stelmach GE, Requin J (eds) Tutorials in motor behaviour. North-Holland, Amsterdam, pp 523–533

Viviani P, Terzuolo CA (1982) On the relation between word-specific patterns and the central control model of typing: a reply to Gentner. J Exp Psychol HPP 8(6):811–813

Wamain Y, Tallet J, Zanone PG, Longcamp M (2011) Static biological motion: influence of motor preferences on visual discrimination of static ellipses. PLoS One 6(1):e15995

Wamain Y, Tallet J, Zanone PG, Longcamp M (2012) Brain response to handwritten and printed letters differentially depend on the activation state of the primary motor cortex. Neuroimage 63(3):1766–1773

Wing AM (1978) Response timing in handwriting. In: Stelmach GE (ed) Information processing in motor control and learning. Academic Press, New York, pp 153–172

Wing AM (2000) Motor control: mechanisms of motor equivalence in handwriting. Curr Biol 10(6):R245–R248